Electronic Supplementary Information

Manuscript ID CE-ART-04-2015-000712

A facile one-step fabrication of novel $WO_3/Fe_2(WO_4)_3!10.7H_2O$ porous microplates with remarkable photocatalytic activities

S 1.1 Synthesis of WO_3:

We fabricated bare WO_3 on the same experimental conditions as that of WO_3-$Fe_2(WO_4)_3!10.7H_2O$ i.e., Take 3 mmol of sodium tungstate dihydrate ($Na_2WO_4.2H_2O$) in 20 ml of deionized water and magnetically stirred the solution for half an hour. During the stirring, 3 mL of 3 M HCl were added drop-wise to the above solution and finally a greenish solution was transferred into a stainless- steel autoclave of 40 mL capacity. The reaction vessel was sealed and heated at 200 ˚C for 24 hours. The autoclave was then allowed to cool at room temperature and the obtained product was several times washed and centrifuged with distilled water and ethanol and then dried at 80 ˚C for 12 hours. The prepared WO_3 have circular round plate-like structure; the morphology, XRD pattern and UV-absorption along with band gap calculation of the sample are shown in Fig. S1below.

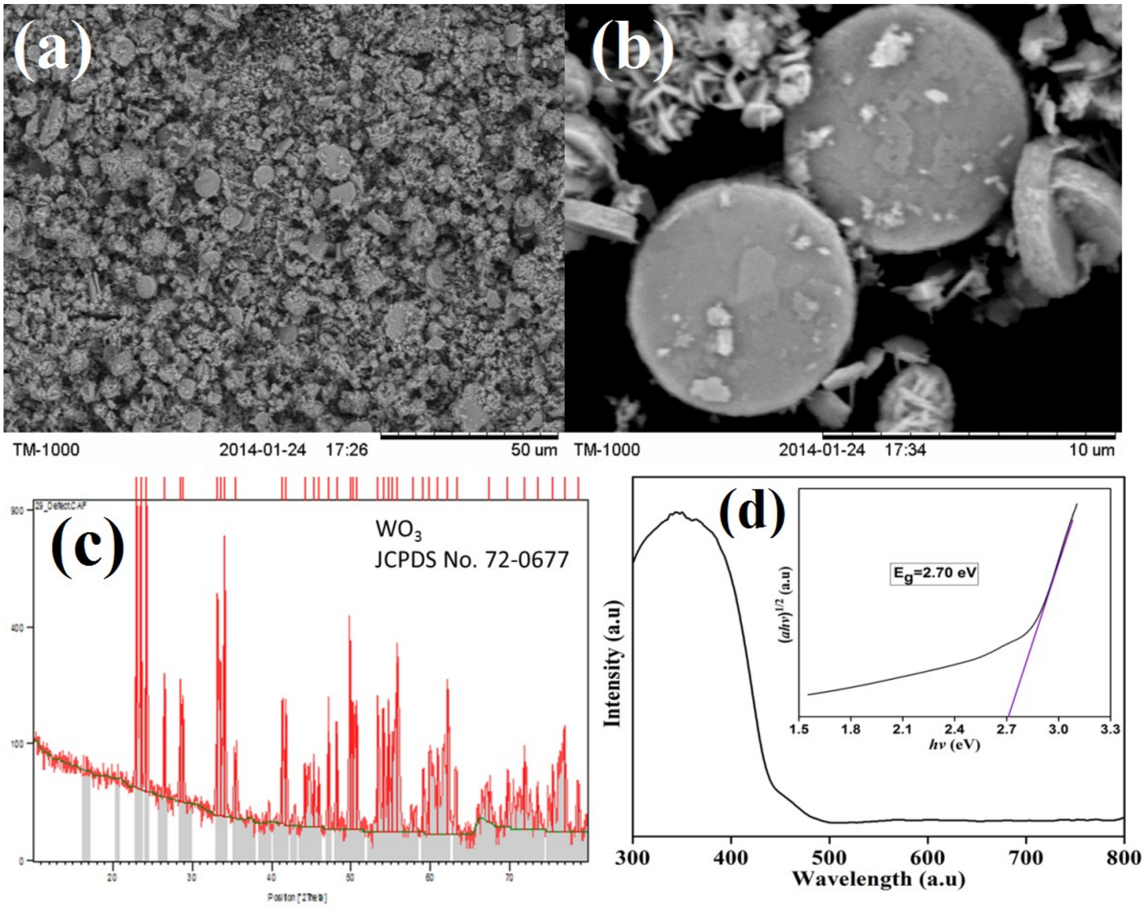

Fig. S1 (a, b) SEM images, (c) XRD pattern and (d) UV- band gap calculation, of WO_3 circular plates

And then we fabricated WO_3-$Fe_2(WO_4)_3$!10.7H_2O by taking 3 mmol of Na_2WO_4.2H_2O and 1 mmlo $FeCl_2$.4H_2O which has pentagonal type plates-like structure. So, it can be proposed that in the synthesis of WO_3-$Fe_2(WO_4)_3$!10.7H_2O, first WO_3 plates formed and then $Fe_2(WO_4)_3$ deposited on these plates. That is the reason we labeled Fig. 3b by mentioning WO_3 plate below and $Fe_2(WO_4)_3$ above that plate.

S 2.1 TG Analysis:

To determine the content of $Fe_2(WO_4)_3$!10.7H_2O in the final product thermogravimetric analysis (TGA) was performed in the temperature range 25 °C to 1000 °C at a heating rate of 10 °C min^{-1} under air conditions. Fig. S2 indicates that there appear two weight losses in the whole process; the first weight loss starts from 185 °C and finished at 480 °C while the second weight loss starts from 540 °C and ends at 640 °C. Since for WO_3, there appears almost no weight loss from room temperature range to 1000 °C [1], so the TGA suggests that $Fe_2(WO_4)_3$!10.7H_2O presents the weight loss in the temperature range 25 °C to 1000 °C which about 6.5 % indicating the weight proportion of iron tungsten oxide hydrate ($Fe_2(WO_4)_3$!10.7H_2O) in the heterostructure system $WO_3/Fe_2(WO_4)_3$!10.7H_2O, and the rest is WO_3.

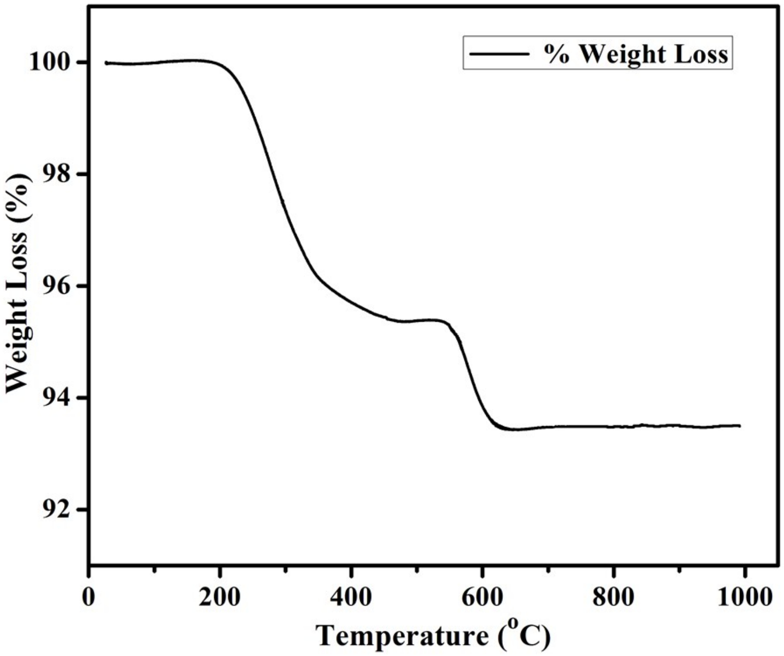

Fig. S2. TG thermograms for heating the $WO_3/Fe_2(WO_4)_3$!10.7H_2O composite from 25 °C to 1000 °C at a heating rate of 10 °C min^{-1}

S 3.1 Synthesis of $Fe_2(WO_4)_3$:

Took 1 mmol of ($Na_2WO_4.2H_2O$), 1 mmol $FeCl_2.4H_2O$ and 1 mmol of NaCl in 22 ml of deionized water in a glass beaker and magnetically stirred the solution for half an hour. During the stirring, added 3 mL of 3 M HCl drop wise to the above solution and again magnetically stirred the solution for half an hour. Finally a thick off white solution was sealed into a stainless-steel autoclave of 40 mL capacity and heated at 200 ˚C for 24 hours. The autoclave was then allowed to cool naturally and the obtained product was several times washed and centrifuged with distilled water and ethanol and then dried at 80 ˚C for 12 hours. Consequently, a yellow color powder was obtained which was preserved for examinations. The XRD pattern and XPS spectrum of the as-synthesized material is given in Fig. S3 (a, b). The morphological structure and UV-absorption along with band gap calculation can be seen in Fig. S3 (c and d).

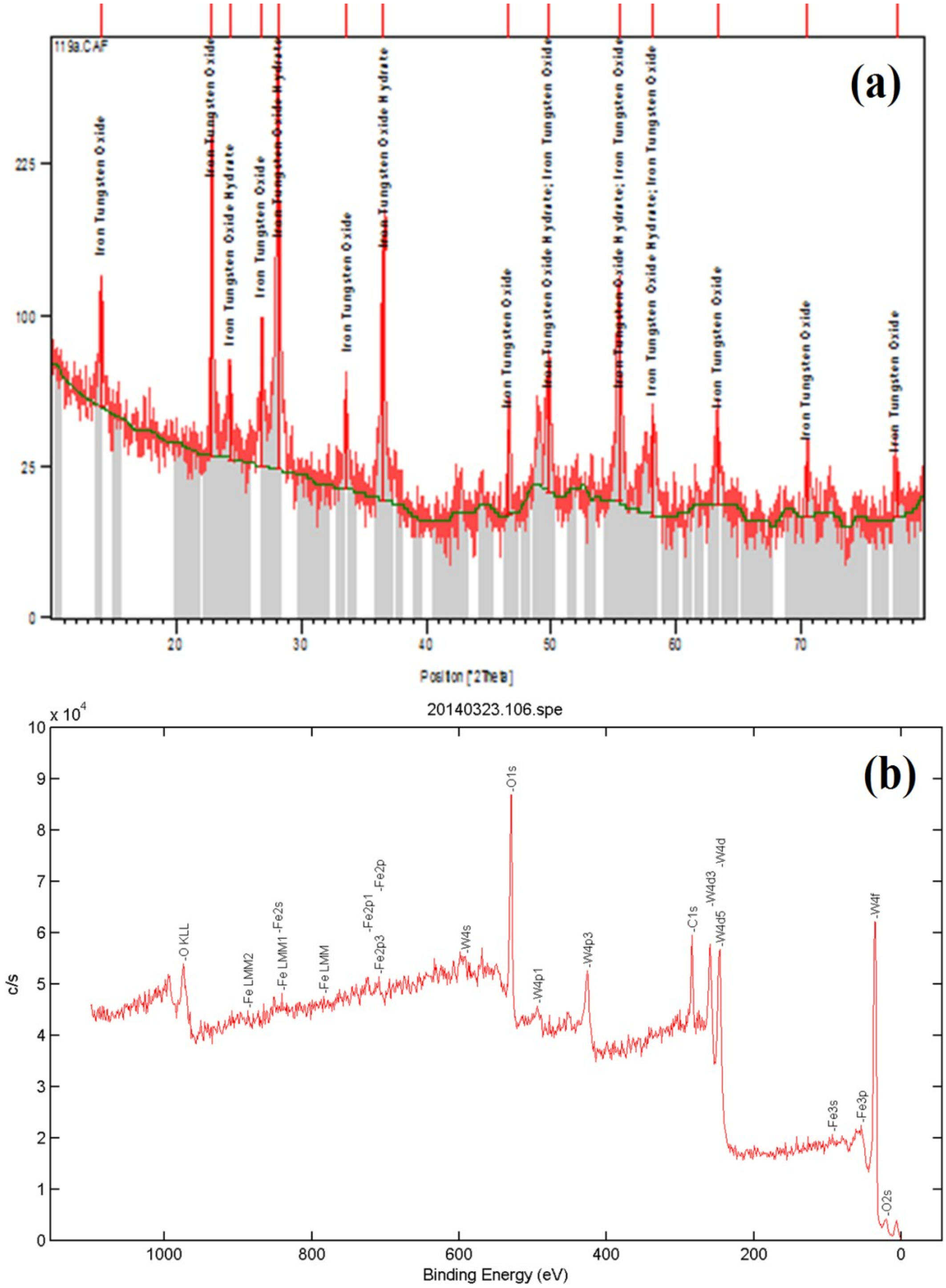

Fig. S3 (a, b) XRD (JCPDS# 23-0309 iron tungsten oxide hydrate, and JCPDS# 38-0200 iron tungsten oxide) pattern and XPS spectrum

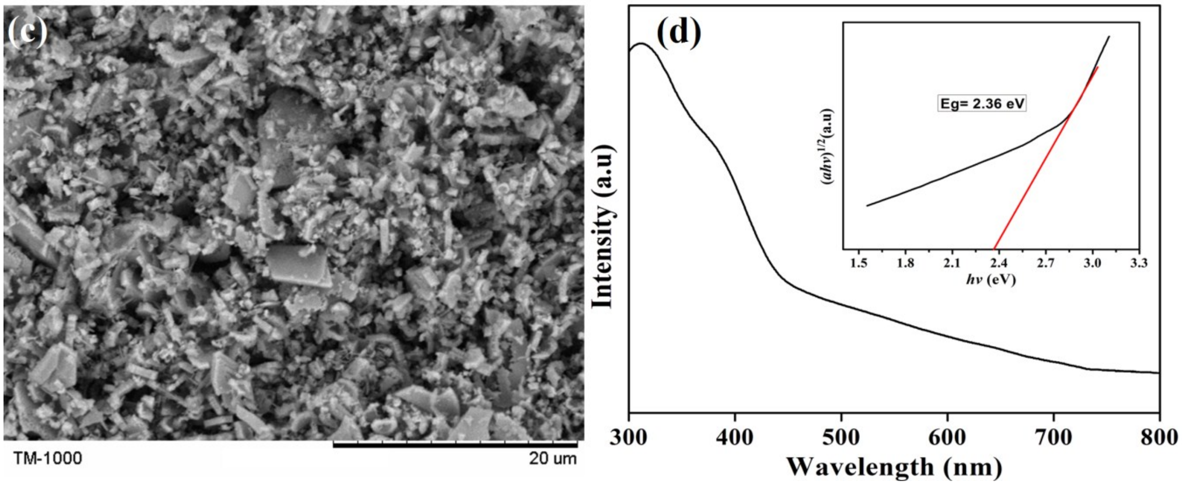

Fig. S3 (c) SEM image and (d) UV-absorption with band gap calculation of $Fe_2(WO_4)_3$

S 3.2 The proposed mechanism for the separation process of photocarriers:

The band gap of the as-prepared materials $Fe_2(WO_4)_3$ and WO_3 was estimated as 2.36 eV and 2.70 eV. The conduction band (CB) edge and valence band (VB) edge were calculated by the following equations [2, 3]:

$$E_{VB} = \chi - E^e + \frac{1}{2}E_g \qquad (1)$$

$$E_{CB} = E_{VB} - E_g \qquad (2)$$

where E_{VB} and E_{CB} are the valence band and conduction band edge potentials respectively, χ is the electronegativity of the semiconductor, which is the geometric mean of the electronegativity of the constituent atoms. The values of χ for $Fe_2(WO_4)_3$ and WO_3 have been calculated as 6.37 eV and 6.59 eV according to literature [4]. E^e is the energy of free electrons on the hydrogen scale (4.5 eV) and E_g is the band gap energy of the semiconductor. On the basis of band gap positions, the band edge potentials of VB and CB for WO_3 are 3.44 eV and 0.74 eV while for $Fe_2(WO_4)_3$ are 3.05 eV and 0.69 eV respectively. The band alignment of the as prepared

$WO_3/Fe_2(WO_4)_3$!10.7H_2O sample with the reference of potential *vs* NHE has been discussed in Fig. S3 (e). Since the CB edge potential (0.69 eV) of $Fe_2(WO_4)_3$ is more active (or at lower potential) than that of WO_3 (0.74 eV); hence, the photogenerated electrons from $Fe_2(WO_4)_3$ may easily transfer to the CB of WO_3 via interface. Similarly, the VB edge potential of WO_3 (3.44 eV) is more positive (or at higher potential) than that of $Fe_2(WO_4)_3$ (i.e., 3.05 eV), therefore, photogenerated holes migrate from the VB of WO_3 surface to the VB of $Fe_2(WO_4)_3$. As a result, a large number of electrons gather on the conduction band of WO_3 surface and holes on the valence band of $Fe_2(WO_4)_3$ surface, which increase the lifetime of charge carriers (or slow down the recombination of photoinduced electron-hole pairs) and enhance the interfacial charge transfer, and finally results in high photocatalytic activity of the $WO_3/Fe_2(WO_4)_3$!10.7H_2O photocatalyst.

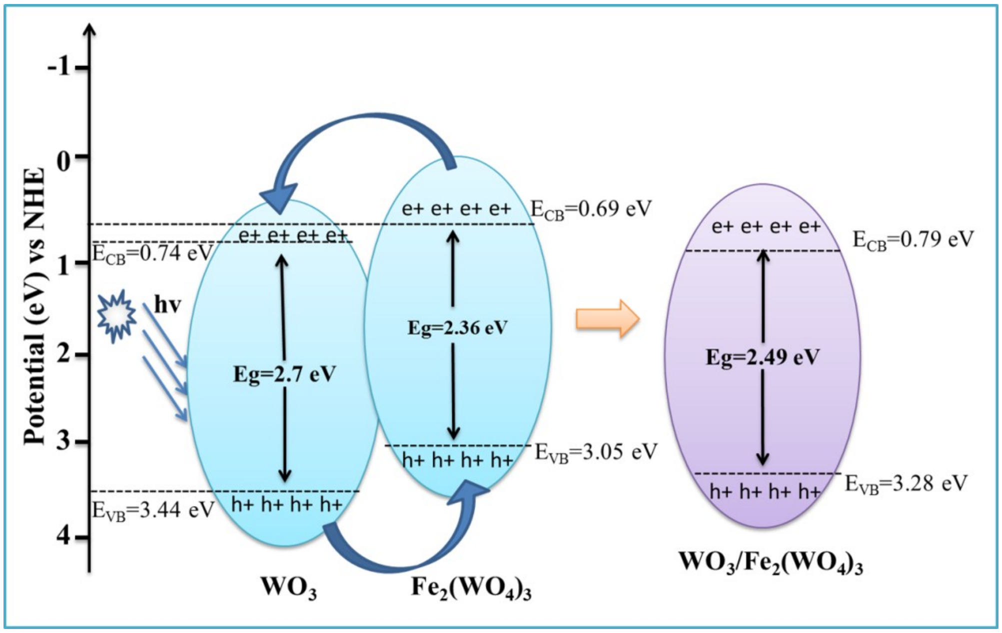

Fig. S3 (e) The proposed mechanism of $WO_3/Fe_2(WO_4)_3$!10.7H_2O for the photogenerated charge carriers under visible-light irradiation.

References:

1. V. Hariharan, S. Radhakrishnan, M. Parthibavarman, R. Dhilipkumar and C. Sekar, *Talanta,* 2011, **85**, 2166–2174.
2. M. Sadakane, K. Sasaki, H. Kunioku, B. Ohtani, R. Abe and W. Ueda, J. Mater. Chem., 2010, **20**, 1811-1818.
3. C. Feng, S. Wang and B. Geng, Nanoscale, 2011, **3**, 3695-3699.
4. R. G. Pearson, Inorg. Chem., 1988, **27**, 734-740.